

## Heat Transfer Enhancement by Using Dimpled Surface

Hemant C. Pisal<sup>1</sup>, Avinash A. Ranaware<sup>2</sup>

<sup>1</sup>Department of Mechanical Engineering, College of Engineering, Phaltan, India.)

<sup>2</sup>Department of Mechanical Engineering, College of Engineering, Phaltan, India.)

**ABSTRACT:** The importance of heat transfer enhancement has gained greater significance in such areas as microelectronic cooling, especially in central processing units, macro and micro scale heat exchangers, gas turbine internal airfoil cooling, fuel elements of nuclear power plants, and bio medical devices. A tremendous amount of effort has been devoted to developing new methods to increase heat transfer from finned surface to the surrounding flowing fluid. Rib turbulators, an array of pin fins, and dimples have been employed for this purpose. An investigation was conducted to determine whether dimples on a heat sink fin can increase heat transfer for laminar airflows. This was accomplished by performing an experimental and numerical investigation using two different types of dimples: 1) circular (spherical) dimples, and 2) oval (elliptical) dimples. Dimples were placed on both sides of a copper plate with a relative pitch of  $S/D=1.20$  and relative depth of  $\delta/D=0.2$  (e.g., circular dimples). For oval dimples, similar ratios with the same total depth and circular-edge-to-edge distance as the circular dimples were used. For those configurations the average heat transfer coefficient and Nusselt number ratio were determined experimentally. For circular and oval dimples, heat transfer enhancements (relative to a flat plate) were observed for Reynolds number range from 600 to 2000 (Reynolds number based on channel height). Moreover, pressure drop, thermal performance and flow characteristic were simulated numerically.

**Keyword:** Laminar flow

### I. INTRODUCTION

The importance of heat transfer enhancement has gained greater significance in such areas as microelectronic cooling, especially in central processing units, macro and micro scale heat exchangers, gas turbine internal airfoil cooling, fuel elements of nuclear power plants, and bio medical devices. A tremendous amount of effort has been devoted to developing new methods to increase heat transfer from finned surface to the surrounding flowing fluid. Rib turbulators, an array of pin fins, and dimples have been employed for this purpose. In case of the electronics industry, due to the demand for smaller and more powerful products, power densities of electronic components have increased. The maximum temperature of the component is one of the main factors that control the reliability of electronic products. Thermal management has always been one of the main issues in the electronics industry, and its importance will grow in coming decades. The use of heat sinks is the most common application for thermal management in electronic packaging. Heat sink performance can be evaluated by several factors: material, surface area, flatness of contact surfaces, configuration, and fan requirements. Although there are a few investigations for the use of dimples under laminar airflow conditions, there exist no experimental data with respect to the use of different dimple shapes for heat sink applications. Therefore, this study evaluated the heat transfer characteristics using two different dimple shapes on a heat sink fin by experimental and numerical methods: 1) circular (spherical) dimples, and 2) oval (elliptical) dimples. The average heat transfer coefficient and heat transfer performance were obtained experimentally. Heat transfer coefficient, pressure drop, thermal performance and flow characteristics were simulated numerically. Several parameters were chosen to evaluate the effects of dimples: Reynolds number ( $ReH$ ), relative channel height ( $H/D$ ), relative dimple depth ( $\delta/D$ ), and turbulent intensity. Many investigations have been conducted for a rectangular channel. Chyu et al. [2] studied the enhancement of surface heat transfer in a channel using two different concavities- hemispheric and tear drop. Concavities serve as vortex generators to promote turbulent mixing in the bulk flow to enhance the heat transfer at  $ReH = 10,000$  to  $50,000$ ,  $H/d$  of 0.5, 1.5, 3.0 and  $\delta/d = 0.575$ . Heat transfer enhancement was 2.5 times higher than smooth channel values and with very low pressure losses that were almost half that caused by conventional ribs turbulators. Moon et al. [3] experimentally studied

the effect of and friction losses in a rectangular dimpled passage with staggered dimples on one wall. The geometry used was  $H/D = 0.37, 0.74, 1.11, 1.49$  and  $ReH = 12,000$  to  $60,000$ . Heat transfer enhancement was roughly 2.1 times greater than the smooth channel configuration with  $H/D$  values from 0.37 to 1.49. The heat transfer augmentation was invariant with the Reynolds number and channel height. The increase in friction factor was 1.6 to 2.0 times less than the smooth channel. The pressure losses also remained approximately constant for the channel height. Mahmood et al [4] studied the flow and heat transfer characteristics over staggered arrays of dimples with  $\delta/D=0.2$ . For the globally average Nusselt number, there were small changes with Reynolds number. Ligrani et al [5] studied the effect of dimpled protrusions (bumps) on the opposite wall of the dimpled surface. Mahmood et al [6] experimentally showed the influence of dimple aspect ratio, temperature ratio, Reynolds number and flow structures in a dimpled channel at  $ReH = 600$  to  $11,000$  and air inlet stagnation temperature ratio of 0.78 to 0.94 with  $H/D = 0.20, 0.25, 0.5, 1.00$ . The results indicated that the vortex pairs which are periodically shed from the dimples become stronger and local Nusselt number increase as channel height decreases. As the temperature ratio  $T_{oi}/T_w$  decreases, the local Nusselt number also increased. Burgess et al [7] experimentally analyzed the effect of dimple depth on the surface within a channel with the ratio of dimple depth to dimple printed diameter, equal to  $\delta/D, 0.1, 0.2, \text{ and } 0.3$ .

## II. EXPERIMENTAL SETUP

A schematic drawing of the facility used for heat transfer measurements is shown in Fig. 1. The average heat transfer coefficient on the plate surface was measured for various rates of airflow through the channel. It consists of an open loop flow circuit. The main components of the test apparatus are a test section, a rectangular channel, a plenum, a calibrated orifice flow meter, a gate valve, and a centrifugal blower. The channel inner cross section dimensions are 33mm (wide) and 105 mm (height). The entrance channel is 1500mm long. The channel was constructed with 8 mm thick acrylic plates with thermal conductivity  $k=0.16\text{W/mk}$  at  $20^\circ\text{C}$  to minimize heat losses. A  $300\times 300\times 450\text{mm}$  plenum with wood was fabricated to stabilize the flow drawn by the blower Figure 3.2 shows the cross section of the test section. All exterior surfaces of the test section are insulated with fiberglass ( $k=0.04\text{W/mk}$ ) to minimize heat losses. Infrared electric heaters model KH-108/5-P (Kapton heater,  $25.4\times 203.2\text{mm}$ , 115 Volts, 40 W total power, pressure sensitive adhesive on one side) is used to provide a constant heat flux to the copper plate. The heaters allowed heat flux through the 5 mm-thick test plate. Power was supplied by an Elenco Precision variable power supply model XP-800, with multi-meters TENMA 72-6685A and 72-6185 used to measure voltage and current into the heater. Fig 3.3 shows the CPU and heat sink with dimples. Only one fin was used to study and quantify the heat transfer enhancement characteristics. For the case of internal heat convection test with a square channel, a uniform heat flux is applied from the bottom of the plate. For this study, heat flux was applied from top of the plate to simulate similar test conditions for an actual heat sink application. Figs 2(a), (b), and (c) present the geometric details of the test surface including dimple geometry. The circular dimpled plate with 11 by 22 dimples the oval (elliptical) dimpled plate with 7 by 22 dimples on each side. The dimples were placed on both sides of the copper plate with a relative pitch  $S/D=1.21$  and a relative depth  $\delta/D=0.2$  for the circular dimples. For the oval dimples,  $S/D=1.21$  and  $\delta/D=0.2$  with same total depth and circular-edge-to-edge distance as the circular dimples. Three test plates were fabricated with 5mm thickness ASTM B152 Electroless Oxygen-Free Copper. Because a flat projected area was used to calculate a heat transfer coefficient and a Nusselt number, the total surface area for each plate was constant. Fig. 2 shows Schematic drawings, (a) the entire test surface of the flat copper plate; (b) the entire test surface of the circular type Al plate with dimple dimensions;(c) the entire test

surface of the oval (elliptical) type copper plate with dimple dimensions. All dimensions are given in mm.

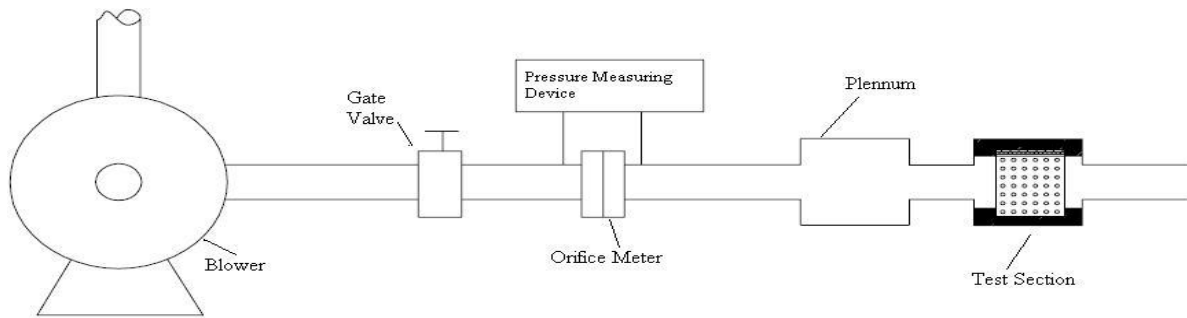


Fig.1. Experimental Set-up

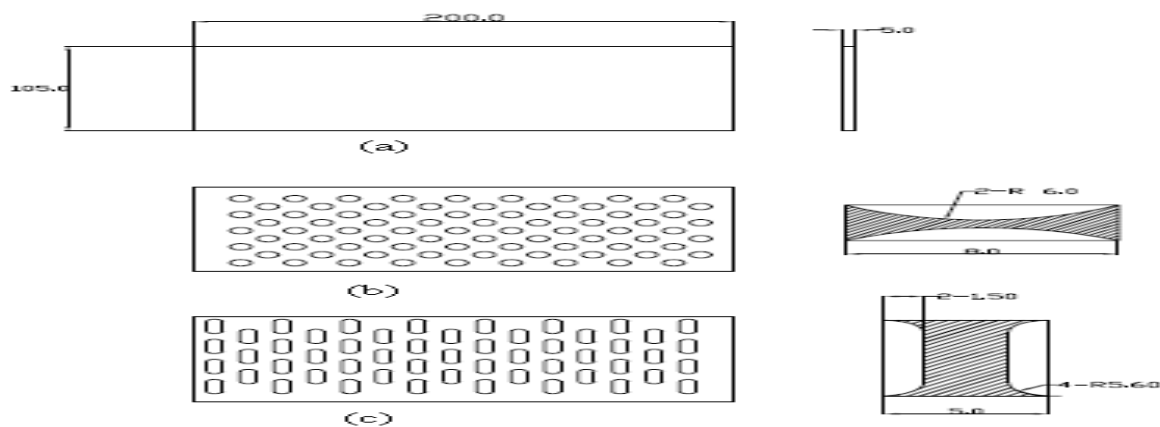


Fig.2. Schematic drawings, (a) the entire test surface of the flat copper plate; (b) the entire test surface of the circular type copper plate with dimple dimensions ; (c) the entire test surface of the oval (elliptical) type copper plate with dimple dimensions. All dimensions are given in mm.

The blower will be turned on and air is forced through the test setup. The flow rate through the test section will be controlled with the help of a valve downstream of the orifice plate. The flow rate will be set in such a way so that the pressure drop across the orifice corresponds to required Reynolds number. After the flow will be set across the test section, the heaters will be turn on and the voltage supplied to the heaters will be roughly set to 15W. According to the temperature of the test plate, voltage and current will be changed. After the measured temperatures will reach a specific value, the voltage will be controlled to an input power 14W. After as time elapse of roughly 6 hours, the temperature of the test plate will reaches steady state. The pressure difference across the orifice will be checked frequently so that the flow rate does not change from the intended value of Reynolds number. At steady state, the temperatures of the test plate will be checked by the data acquisition system. The pressure difference across the orifice plate and the pressure across upstream of the orifice plate will be measured. The voltage supplied to the heater and the corresponding current will be taken to calculate the heat supplied to the test plate. The temperatures of the inlet air into the test section and into the orifice plate will also check. The objective of this investigation is to study the heat transfer characteristics using dimples at low Reynolds number flow conditions. An average heat transfer coefficient will be calculated from the net heat transfer per unit area, the average temperature of the plate, and the bulk mean air temperature. To quantify the average heat transfer coefficient, the following expression will be used:

$$h = \frac{Q_{net}}{A_s(T_w - T_b)} = \frac{Q_{total} - Q_{loss}}{A_s(T_w - T_b)} \quad \text{--- (1)}$$

Where the net heat flux ( $Q_{net}$ ) is the electrical power supplied to the heater ( $Q_{total}$ ) minus the heat loss from the test section ( $Q_{loss}$ ). The surface area of the plate where the heat convection occurs,  $T_w$  is a steady-state wall temperature and  $T_b$  is a mean bulk temperature.

$$Q_{total} = V \cdot I \quad \text{-----} \quad (2)$$

$Q_{total}$  will be calculated from  $V$ , input voltage and  $I$ , the input current to the flexible heater.  $Q_{loss}$  will be calculated by running the test without air flow under the same wall temperature obtained as the actual test with air flow. The amount of power input is the heat loss  $Q_{loss}$ . For the general case, heat loss is calculated to be roughly 5~10%. A mean bulk temperature,  $T_b$ , will be determined by Eq. 3 where  $T_{b, inlet}$  is the inlet bulk temperature and  $T_{b, outlet}$  is the outlet bulk temperature that can be calculated from Eq. 4:

$$T_b = \frac{T_{b, inlet} + T_{b, outlet}}{2} \quad \text{-----} \quad (3)$$

$$T_{b, inlet} = T_{b, outlet} + \frac{Q_{total} - Q_{loss}}{mC_p} \quad \text{----} \quad (4)$$

### III. UNCERTAINTY

The uncertainty of the average heat transfer coefficient depends on the uncertainties in the average wall temperature, bulk air temperature difference, and the net heat input for each test section. This uncertainty increases with decreasing both the average wall temperature to bulk air temperature difference and the net heat flux. Based on a confidence level of 95% described by Kline and McClintock, uncertainty value of  $\pm 0.5\%$  for all properties of the air, and  $\pm 0.5\%$  for all physical dimensions were used. Based on the maximum uncertainties for pressure at the orifice flow meter, and the pressure drop across the orifice of  $\pm 1.0\%$  and  $\pm 4.1\%$ , respectively, the maximum uncertainty of the air mass flow rate was calculated to be  $\pm 2.8\%$ . The corresponding maximum uncertainty of the Reynolds number was  $\pm 2.9$ . The uncertainty for the power input and heat loss were found to be  $\pm 3.1\%$  and  $\pm 5.4\%$ , respectively, and those for the average wall and bulk temperatures  $\pm 3.0\%$  and  $\pm 3.5\%$ , respectively. With these values, the uncertainty of the Nusselt number was calculated to be  $\pm 7.8\%$ .

### IV. MATHEMATICAL MODEL

Fluid flow and heat transfer in a channel can be described mathematically by using three fundamental laws: The Principle of Mass Conservation, The Principle of Momentum Conservation and The Principle of Energy Conservation. Numerical studies were conducted to determine the heat transfer and velocity profiles on the copper plate for laminar airflow in a rectangular channel. The dimensions of the Al plates were the same as the experimental specimens. The entrance channel is 600mm long rectangular channel with a flow cross section of 33 mm (width) by 105mm (height). The exit channel is 1500 mm long rectangular channel with a flow cross section of 33 mm (width) by 105mm (height). Because of symmetry in the flow direction, the numerical model was only solved for half of the channel and plate. This was helpful in reducing the need for more memory and the required processing time, which was especially critical for modeling the complex and detailed geometries of the dimpled heat sinks. Tetrahedral elements aligned with the flow direction were used to reduce the numerical dissipation errors and improve the quality of numerical predictions. Fine grids were employed for near-wall and dimpled surfaces to resolve the high gradients encountered in these region. The numbers of finite volume hexahedral cells employed for the entire flow domain and each region are shown in Table1. The SIMPLE (Semi-Implicit Method for Pressure-Linked Equations) algorithm, along with a structured grid, was used to couple the pressure and velocity fields. The second-order upwind interpolation scheme and second-order spatial discretization scheme were used to reduce numerical errors. Three different sets of grids were tested for grid independence of the circular dimpled plate: 6 by 8, 8 by 13, 10 by 16, and 6 by 8 type were employed for circular and oval type dimple.

### V. RESULTS

This investigation presents both experimental and numerical studies for the heat transfer characteristics for a heat sink with laminar airflow conditions. This was conducted with two different types of dimples: 1) circular (spherical) dimples, and 2) oval (elliptical) dimples. The average heat transfer coefficient and Nusselt

number ratio were obtained experimentally. Heat transfer, pressure drop, thermal performance and flow characteristics were numerically simulated. Experiments using aluminum plates with a flexible heater were conducted to obtain Nusselt number ratio for a heat sink with dimpled surfaces in laminar airflow. Three different copper plates were fabricated and used to obtain the average heat transfer coefficient: flat, circular, and oval dimpled plates. Dimples were placed on both sides of the aluminum plate. Each plate was placed in the middle of the rectangular channel and a uniform heat flux was applied from the top of the plate. The flat plate was used as baseline data. Average heat transfer coefficients were calculated for four different Reynolds numbers based on channel height,  $Re_H$  from 500 to 2000 with a uniform heat flux of  $1.4 \times 10^4 \text{ W/m}^2$ . Fig 3 shows the heat transfer coefficients for three different copper plates based on the flat projected area. The heat transfer coefficients increased with increasing airflow rate. The results showed that the heat transfer coefficients for the circular and oval dimpled plates were higher than that of the flat plate for all airflow conditions. In Fig 4, the experimental results of the heat transfer enhancement characteristics for the circular and oval dimpled plates are presented. At very low flow velocity ( $Re_H=500$ ),  $N_u/N_{u0}$  values for circular and oval type dimpled plate were less than 1.02. For  $Re_H$  from 750 to 1650,  $N_u/N_{u0}$  values for both circular and oval type cases are around 1.06 regardless of  $Re_H$ .

The same geometries and test conditions as with the experimental specimens were used to simulated heat transfer coefficient, pressure drop, thermal performance, and flow characteristics using FLUENT version 6.2.16.

All experimental test runs were selected for comparison with the numerical predictions. Geometrical features of the numerical model were the same as those of the experiments. Fig 5 shows the heat transfer coefficients comparison of the experimental and numerical models for the four different Reynolds numbers of 500, 750, 1000, 1250, 1500, 1750 and 2000. The results of the numerical simulations were similar with those of the experiments; the heat transfer coefficients of the numerical results were smaller than those of the experimental results. The reason for the lower heat transfer coefficients for the numerical results is that the boundary condition of the numerical study was different with the boundary condition of the experiment. In case of the numerical study, heat loss to the outside surroundings was not included. If the boundary condition for the numerical study was applied the same as the experiment, the difference between numerical and experimental results should be smaller than the obtained. Fig 7 compares the thermal performance factor for two different dimpled plates: circular and oval dimpled plate. Both cases showed that the thermal performance factor increases with increasing mass flow rate. The thermal performance factor for the oval dimpled plate increased from 1.0 to 1.21. The thermal performance factor for the circular dimpled plate increased from 1.0 to 1.12. The factor for the oval type dimpled plate was larger than that of the circular dimpled plate for all cases. The flow structure was investigated by analyzing the numerical model. The stream wise sectional view, span wise sectional view, top view over a dimple, and top view inside of a dimple were plotted which enabled the flow structure to be visualized. Fig. 8 shows the schematic diagram for circular and oval dimpled plates, which were employed. Fig 8 shows the stream wise sectional view of the flat plate for  $Re_H=500$  and  $Re_H=1800$ . In Fig. 8, the streamlines are displayed for each case. In the case for  $Re_H=1800$ , stronger and larger recirculation regions exist for both the upstream and downstream region. Reattachment is evident at the landing area of the dimples at the downstream regions. The flow reattachment enhances the local convection heat transfer. On the other hand, a recirculation zone reduces heat convection because the flow is trapped in that zone. Using an experimental method, the heat transfer coefficient of the three copper plates was calculated. The value was increased with increasing mass flow rate. At very low flow velocity (Reynolds number based on channel height  $Re_H=500$ ), the ratio for  $N_u/N_{u0}$  for circular and oval type dimpled plate is less than 1.02. For Reynolds number from 750 to 2000,  $N_u/N_{u0}$  ratios for both circular and oval cases were approximately around 1.11 regardless of  $Re_H$ . Numerical studies for the same geometries and test conditions with the experimental study were conducted. The heat transfer coefficients of the numerical results are similar with those of the experiment results, but the heat transfer coefficients of the numerical results are smaller than those of the experiments. The pressure drops of the dimpled plates for a laminar airflow are either equivalent to, or less than values produced in a flat plate with no dimples. As the airflow velocity gets faster, the thermal performances of circular and oval plates increased. Generally, the thermal performance of the oval type plate was higher than that that of the circular dimples. Both the circular and oval dimpled plates show that a prime vortex pair results from the recirculation region inside of the dimples. Primary vortexes are positioned in the upstream of the dimple. From each side of dimples, the

second vortex flows are observed. The reattachment of the central and secondary vortex flow occurred at the trailing edge.

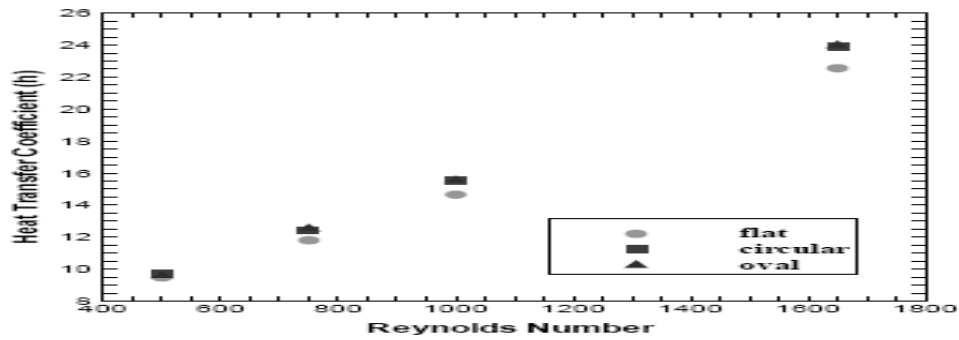


Fig.3. Heat transfer coefficient for the Al plates

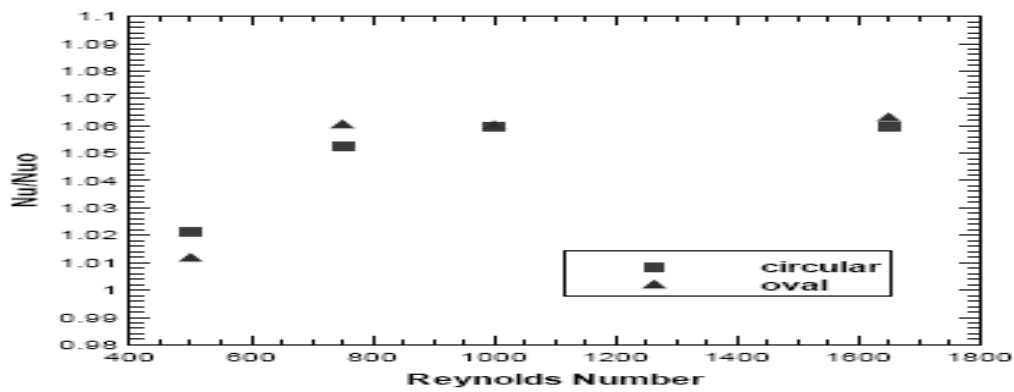


Fig.4. Heat transfer enhancement on the dimple plates

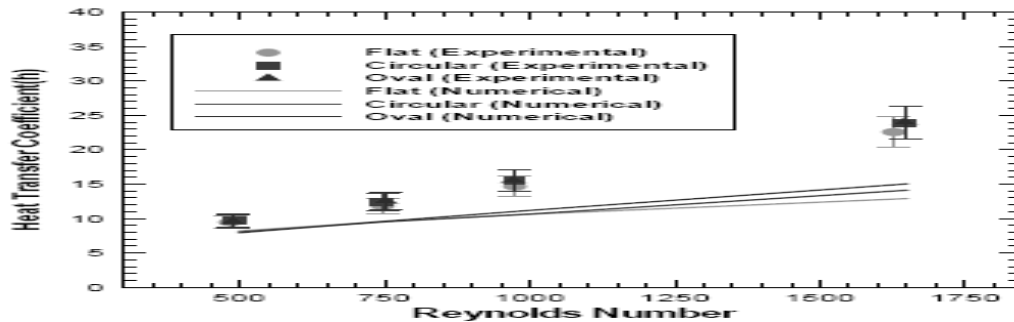


Fig.5. Heat transfer enhancement on the dimple Plates

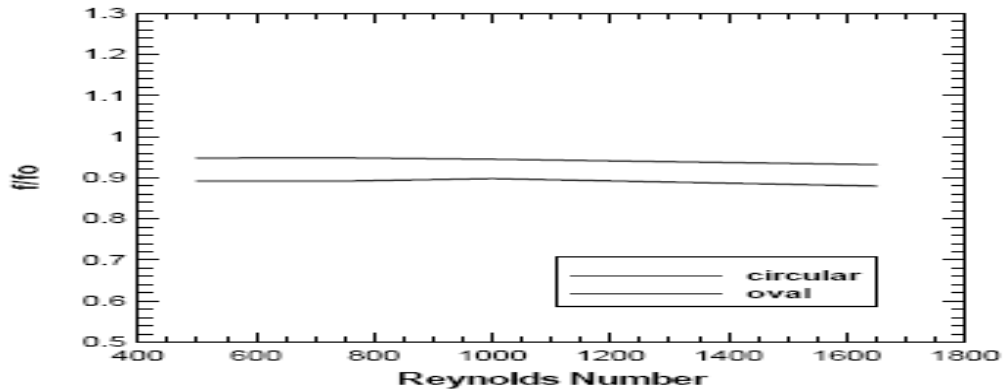


Fig.6. Friction factor ratio, f/f0

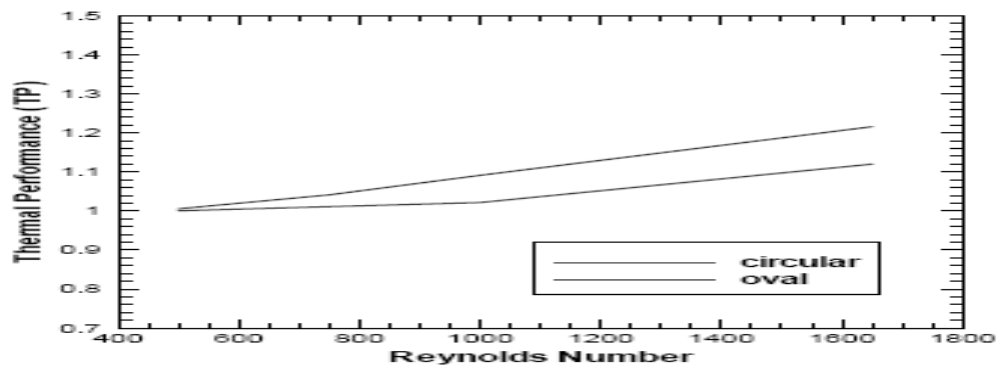


Fig.7. Thermal performance for the dimple plates

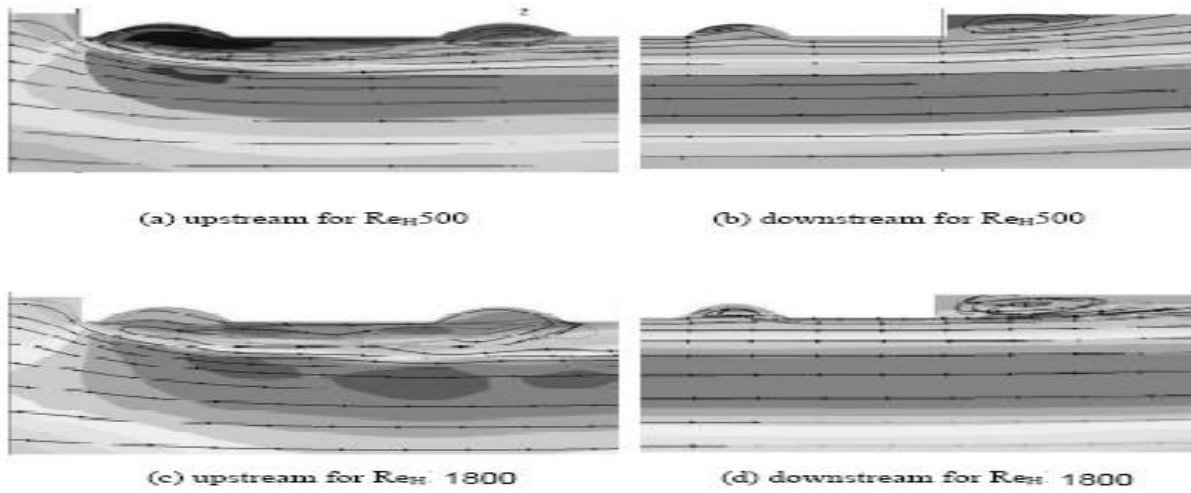


Fig.8a. Streamline of upstream and downstream for the dimpled plates

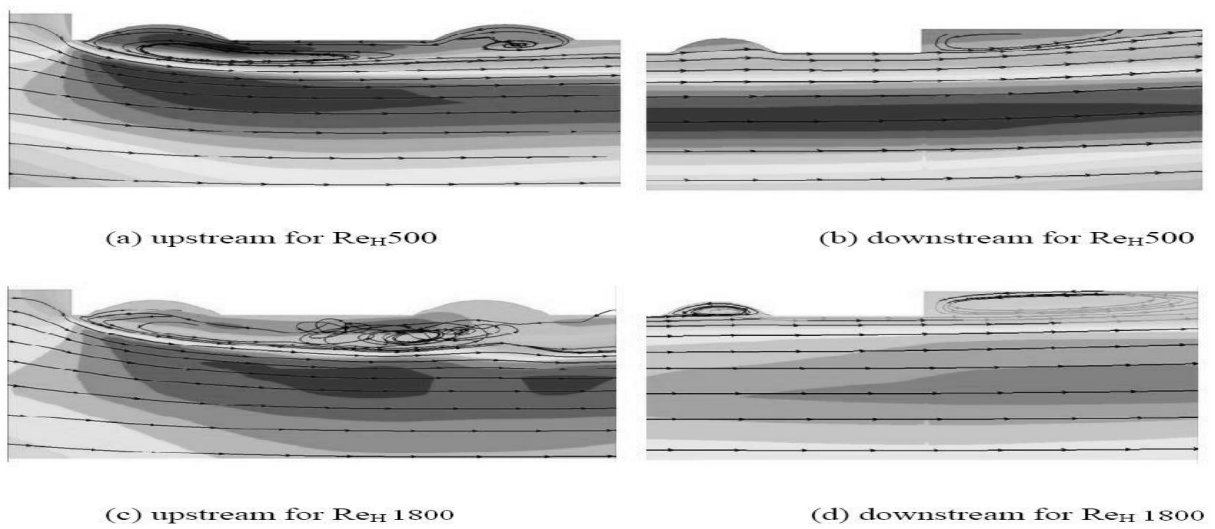


Fig.8b. Streamline of upstream and downstream for the dimpled plates

## VI. CONCLUSION

This investigation presents experimental and numerical results for the heat transfer characteristics of a heat sink for laminar airflow conditions using two different types of dimples. The average heat transfer and heat transfer enhancement were obtained experimentally. Heat transfer, pressure drop, thermal performance and flow conditions were numerically simulated. Experiments using aluminum plates with a flexible heater were conducted to obtain heat transfer characteristics for a heat sink with dimpled surfaces in laminar airflow. Three different aluminum plates were fabricated and used to obtain the average heat transfer: flat, circular, and oval dimpled plates. Dimples were placed on both side of the aluminum plate. Each plate was located in the middle of the rectangular channel and a uniform heat flux was applied from the top of the plate. The flat plate was used for baseline data. The findings of this experimental study are summarized as follows:

1. The heat transfer coefficient of the three aluminum plates increased with increasing mass flow rate,
2. At very low flow velocity (Reynolds number based on channel height  $Re_H=500$ ), the ratio for  $N_u/N_{u0}$  for circular and oval type dimpled plate is less than 1.02,
3. For Reynolds number from 750 to 2000,  $N_u/N_{u0}$  ratios for both circular and oval cases were approximately around 1.11 regardless of  $Re_H$ . The same geometries and test conditions with the experimental study were used to simulate heat transfer coefficient, pressure drop, thermal performance, and flow by using FLUENT version 6.2.16. The findings of this numerical study are summarized as follows:

1. The heat transfer coefficients of the numerical results are very similar with those of the experiment results, but the heat transfer coefficients of the numerical results are smaller than those of the experiments,
2. The pressure drops of the dimpled plates for a laminar airflow are either equivalent to, or less than values produced in a flat plate with no dimples. The pressure drop of the oval type dimpled plate is smaller than that of the circular type dimpled plate,
3. As the airflow velocity gets faster, the thermal performances of circular and oval plates increased. Generally, the thermal performance of the oval type plate was higher than that that of the circular dimples,
4. Both the circular and oval dimpled plates show that a prime vortex pair results from the recirculation region inside of the dimples. Primary vortexes are positioned in the upstream of the dimple. As the airflow gets faster, the primary vortexes are also extended in the downstream direction and gets lager in strength. The oval type plate has lager primary vortexes than the circular plate at the same airflow condition.

### Nomenclature:

$A_S$  = surface area [ $m^2$ ]

$H$  = channel height [m]

$D$  = dimple print diameter [m]

$I$  = current supplied the heater [A]

$T_w$  = average wall temperature [K]

$T_b$  = mean bulk temperature [K]

$T_{b, inlet}$  = inlet bulk temperature [K]

$T_{b, outlet}$  = outlet bulk temperature [K]

$C_p$  = specific heat [K]

$N_u$  = overall average Nusselt number

$N_{u0}$  = overall average Nusselt number of a flat plate

$f$  = friction factor

$f_0$  = friction factor of a flat plate

$K$  = thermal conductivity [ $Wm^{-1}K^{-1}$ ]

$m$  = mass flow rate of air [ $kgs^{-1}$ ]

$S$  = dimple pitch [m]

$h$  = average heat transfer coefficient [ $Wm^{-2}k^{-1}$ ]

$Q_{total}$  = heat transfer from heater [W]

$Q_{loss}$  = extraneous heat loss [W]

$Q_{net}$  = net heat transfer rate [W]

$V$  = voltage across the heater [V]

### Greek Symbols

$\rho$  = density of air [ $\text{kgm}^{-2}$ ]

$\delta$  = dimple depth [m]

### References:

- [1] P.W. Bearman and J.K. Harvey, *Control of circular cylinder flow by the use of dimples*, *AIAA J.* 31 (1993) 1753-1756.
- [2] M.K. Chyu, Y. Yu, H. Ding, J.P. Downs and F.O. Soechting, *Concavity enhanced heat transfer in an internal cooling passage*, *International Gas Turbine & Aeroengine Congress & Exhibition ASME paper 97-GT-437*.
- [3] H.K. Moon, T. O`Connell and B. Glezer, *Channel height effect on heat transfer and friction in a dimpled passage*, *J. Gas Turbine Power* 122 (2000) 307-313.
- [4] G.I. Mamood, M.L. Hill, D.L. Nelson, P.M. Ligrani, H.K. Moon and B. Glezer, *Local heat transfer and flow structure on and above a dimpled surface in a channel*, *J. Turbomachinery* 123 (2001) 115-123.
- [5] P.M. Ligrani, G.I. Mamood and M.Z. Sabbagh, *Heat transfer in a channel with dimples and protrusion on opposite walls*, *J. Thermophys. Heat Transfer* 15 (3) (2001) 275-283.
- [6] G.I. Mahmood and P.M. Ligrani, *Heat Transfer in a dimpled channel: combined influences of aspect ratio, temperature ratio, Reynolds number, and flow structure*, *Int. J. heat Mass Transfer* 45 (2002) 2011-2020.
- [7] N.K. Burgess and P.M. Ligrani, *Effects of dimple depth on channel nusselt numbers and friction factors*, *J. Heat Transfer* 127 (8) (2005) 839-847.
- [8] R.S. Bunker and K.F. Donellan, *Heat transfer and friction factors for flow inside circular tubes with concavity surfaces*, *J. Turbomachinery* 125 (4) (2003) 665- 672..